

See discussions, stats, and author profiles for this publication at: <https://www.researchgate.net/publication/231710029>

# A Novel Approach for Preparing Single-Layer Molecularly Doped Electroluminescent Polymer Thin Films

ARTICLE *in* MACROMOLECULES · SEPTEMBER 1998

Impact Factor: 5.8 · DOI: 10.1021/ma9807771

---

CITATIONS

13

---

READS

15

4 AUTHORS, INCLUDING:



Jwo-Huei Jou

National Tsing Hua University

158 PUBLICATIONS 2,062 CITATIONS

SEE PROFILE

# A Novel Approach for Preparing Single-Layer Molecularly Doped Electroluminescent Polymer Thin Films

Weng-Kou Wen, Jwo-Huei Jou,\* Hua-Shu Wu, and Chien-Li Cheng

Department of Materials Science and Engineering, National Tsing Hua University, Hsin-Chu, Taiwan 30043, R.O.C

Received May 14, 1998; Revised Manuscript Received July 21, 1998

**ABSTRACT:** A single-layer molecularly doped electroluminescent (OEL) polymer thin film has been prepared via a vapor codeposition process. The presented method may be conveniently applied to many dye-doped polymer thin film systems yet without having to go through existing complicated conventional synthesis and fabrication processes. This method, proven in this work to be feasible experimentally, was executed by simultaneously codepositing an EL active dye, a hole-transporting molecule triphenyl-diamine derivative (TPD), and two polyimide thin film forming monomers on an indium–tin oxide (ITO) substrate. Carrier injection was provided from an ITO anode and a thermally evaporated aluminum electrode. Electron–hole recombination and the green light in EL spectra, with an emission maximum at 515 nm, were triggered at a driving voltage of 14 V. Two primary degradation behaviors were identified. First, hydrolysis of the thin films led to the reduction in EL intensity. Second, nonuniform structure formation of the top Al metal in the Al and codeposition film interface caused reduction in the active emission area and increased the driving voltage required.

## Introduction

Organic electroluminescent (OEL) devices are popular for their potential applications in large-area, flat-panel, and high-luminance full-color displays, utilizing low driving voltage, either as backlighting sources or directly as emitters in emissive displays.<sup>1–13</sup> Tang and Vanslyke were the first to report on the high-performance EL devices composed of a vacuum-sublimed double-layer dye film (emissive and hole-transport layers).<sup>1</sup> Since then, various multilayered structure devices, fluorescent dyes, and electrode materials have been studied to improve the efficiency and stability of the devices.<sup>3–7</sup>

Recently, to simplify the fabrication process and to enhance the structural stability of the devices, two types of single-layer EL devices have been proposed.<sup>8–14</sup> The first is a device made with a single compound that must perform three functions: hole transport, electron transport, and light emission. Also, studies of such devices, using conjugated polymer, are drawing significant attention because they are free of problems related to crystallization, aggregation, or heat stability. These problems have so far posed factors that are detrimental to the quality of evaporated films made with low molecular weight compounds.<sup>14</sup> The second type of device is derived by incorporating the properties of different materials into a thin film, that is mixing all hole-transport, electron-transport, and luminescent materials together. This device possesses the advantage in the selection of materials and the freedom of device design with respect to the first type device. In the development of a device made with a single-layer EL, it is becoming evident that such a device is capable of providing a comparable standard of performance as those with multilayered structures.

Devices obtained from using multiple compounds, including dye-doped polymer thin film system, are conventionally prepared by the solvent-dependent method

such as spin-coating or casting. These methods, although convenient, have been proven to be difficult for obtaining a large-area thin and uniform pinhole-free film.<sup>15–19</sup> In addition, the films formed by the above methods may be easily contaminated by various impurities in the solvents used or in the solutes applied. The impurities, as known, may significantly reduce the luminescence efficiency of the devices and, accordingly, should be carefully minimized so that long lifetime and high performance can be achieved.<sup>15,16</sup> An alternative to overcoming the aforesaid drawbacks is to use the vapor deposition polymerization (VDP) technique. The advantage of this dry process is that much less impurities can be expected and the film thickness can be easily controlled as well.<sup>17,20–21</sup>

The purpose of this study is to present a new approach that would enable many polymeric materials to become feasible matrixes and many OEL-active molecules to be the desired dopants for making numerous tailorable OEL thin films. This can be done by simultaneously codepositing an EL-active molecule, a hole-transporting material, and polymer matrix forming monomers on an indium–tin oxide (ITO) glass substrate in a vacuum chamber. In the following sections, we will first reveal the experimental procedures regarding the prospects of accomplishing a codeposition process. Next we will characterize the devices that we have fabricated and then observe the degradation processes of these devices, by using Fourier transform infrared (FTIR) spectrometry and atomic force microscopy (AFM).

## Experimental Section

**Materials.** Figure 1 shows the molecular structures of the materials used and configuration of the OEL device fabricated. In this experiment, tris(8-quinolinolato)aluminum(III) complex (Alq3) was used as the green light-emitting material and *N,N*-diphenyl-*N,N*-bis(3-methylphenyl)-1,1'-biphenyl-4,4'-diamine (TPD) was used as a hole-transport material. They were purchased from Tokyo Kasei Chemical Co., Inc. The polymer thin film forming monomers were pyromellitic dianhydride (PMDA), which was purchased from Chrisken Co.,

\* To whom correspondence should be addressed.

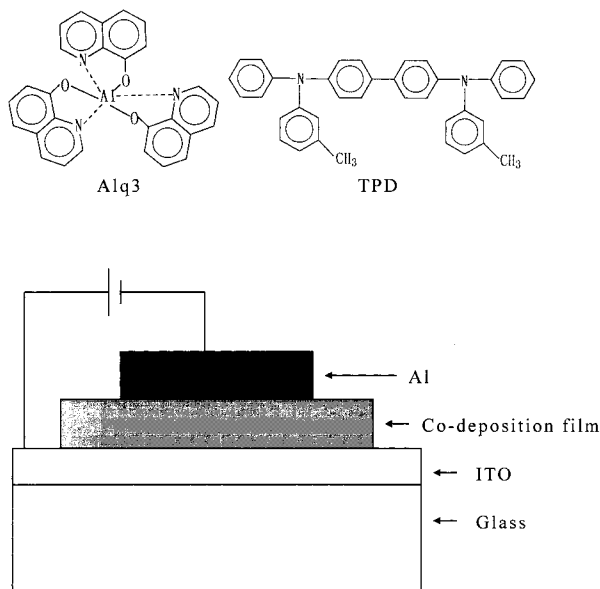


**Figure 1.** Configurations of the presented EL device and the EL-active molecules used.

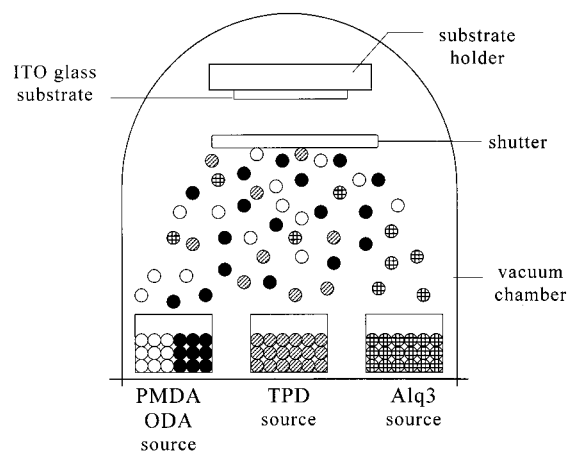


**Figure 2.** Schematic diagram of the vapor deposition polymerization (VDP) system.

Inc., and 4,4'-diaminodiphenyl (ODA), which was purchased from Tokyo Kasei Kogyo Co., Ltd. These materials were used as received.

**Vapor Deposition Polymerization.** Figure 2 shows the schematic diagram of the vapor deposition polymerization (VDP) system. Due to space limitation in the current system, only three sets of source boats were equipped: one for PMDA and ODA monomers, one for TPD, and the final one for the light-emitting fluorescent dye. The single-layer OEL polymer thin films were prepared by simultaneously codepositing the light-emitting molecule, the hole-transporting molecule and the two polymer thin film forming monomers onto an ITO glass substrate using thermal evaporation. Evaporation of the PMDA and ODA monomers was started at 100 °C and stopped at 150 °C with a ramp rate of 6.7 °C/min. The Alq3 molecule was started at 140 °C and stopped at 185 °C with a ramp rate of 7.5 °C/min, and that of the TPD molecule was started at 150 °C and stopped at 180 °C with a ramp rate 5 °C/min. In this study, prior to the deposition process, the source boat was preheated to 10 °C below the starting deposition temperature. This procedure allowed the source boat to be ramped up smoothly. The deposition process began in a vacuum of  $5 \times 10^{-5}$  Pa.

**Preparation of the Organic EL Device.** The substrate used for preparing the OEL device was a precleaned indium-tin oxide (ITO) ( $5 \times 2.5$  cm<sup>2</sup>) conductive glass with a sheet resistance of 80  $\Omega$ /cm<sup>2</sup>. The single-layer EL polymer thin film

was then deposited onto the ITO glass substrate. After the thermal curing process, the top electrode of the Al metal (6000 Å) was then deposited by thermal evaporation in a vacuum of  $4 \times 10^{-6}$  Pa. The emitting area was  $0.5 \times 0.5$  cm<sup>2</sup>.

**Curing.** Thermal curing of some of the as-deposited samples was carried out in a vacuum of  $5 \times 10^{-5}$  Pa after the deposition process. They were elevated to 150 °C at a ramp rate of 2 °C/min and held for 1.5 h before cooling.

**Characterization.** The deposition rates of monomers and molecules were determined by using a Maxtek TM-200R quartz oscillation thickness monitor to acquire the optimized deposition conditions for preparing the codeposited films. The relative amounts of the two monomers and molecules were calculated according to the predetermined deposition rates.

The structure and composition of the resultant films were characterized using Fourier transform infrared (FTIR) spectrometry. The FTIR experiment was performed using a Bomem DA 3002 spectrometer with a resolution of 2 cm<sup>-1</sup>. The spectra, with wavenumbers ranging from 500 to 2000 cm<sup>-1</sup>, were recorded.

A JASCO FR-770 spectrometer was employed to obtain both the photoluminescence and electroluminescence spectra of the resultant devices. Measurement of the  $I$  (current)– $V$  (voltage) curve of the devices was carried out using the programmable Keithley 237. The electroluminescence intensity of the device was measured with a Minolta luminance meter LS-100 at room temperature. All the measurements were carried out in ambient conditions.

**Interface Topology Investigation.** The topology of the interface of the Al electrode and the codeposited polymer thin film was investigated using an atomic force microscope (AFM) of the Nanoscope III system (Digital Instruments Inc.). The root-mean-square (rms) roughness values were determined on the basis of a  $1 \times 1$   $\mu$ m area. The specimens were prepared by immersing the devices in a polyimide etching solution until the Al films peeled off. The Al films were subsequently cleaned using deionized water and then placed on a plate glass substrate with its interfacial side up. The specimens were then dried in a vacuum chamber before measurement.

## Results and Discussion

Figure 3a shows the deposition rates of the PMDA and ODA monomers as a function of evaporation temperature. The PMDA monomer, weighted 0.1 g, began to evaporate markedly at 50 °C at  $5 \times 10^{-5}$  Pa. Its deposition rate increased as the temperature increased until it reached a maximum reading at 120 °C. The ODA monomer, weighted 0.06 g, evaporated markedly at 45 °C and had a maximum deposition rate at 124 °C. Declination of the deposition rates, after reaching the maxima, resulted from depletion of the monomer sources added.

To achieve a high degree of polymerization, it is imperative to accurately control the stoichiometric ratio of the PMDA and ODA monomers. In Iijima's study,<sup>22</sup> deposition of the monomers had been fixed at constant temperatures, e.g., 180 °C for PMDA and 160 °C for ODA. Since in such a system a significant amount of the molecules would be lost before reaching the desired constant temperature and because our system is limited, we performed the deposit by using temperature ramping. Reasonably good single-layer EL thin films had been obtained by codepositing the PMDA and ODA monomers from 100 to 150 °C with a ramp rate of 6.7 °C/min. The molar ratio of ODA to PMDA was calculated to be 1.2 at the beginning of the deposition process and 0.9 at the end. The average molar ratio of ODA to PMDA in the resultant thin films was estimated to be 1.05.

**Doping via Codepositon.** Deposition of the Alq3 molecule, weighted 0.08 g, was started at 140 °C and

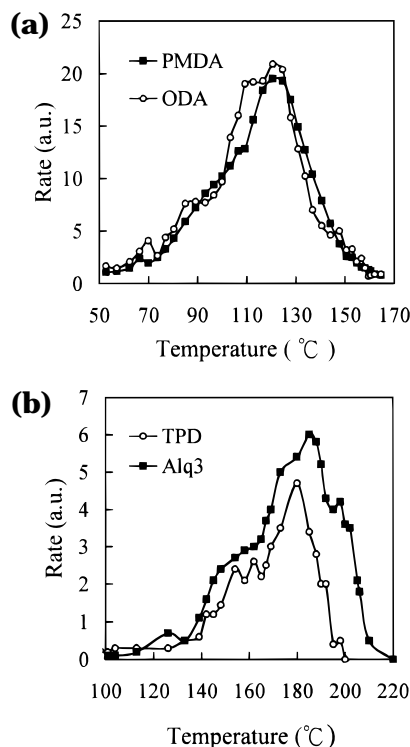


**Figure 3.** Deposition rates of (a) the PMDA and ODA monomers and (b) the Alq3 and TPD molecules as a function of temperature.

stopped at 185 °C with a ramp rate of 7.5 °C/min, and the TPD molecule, weighted 0.02 g, was started at 150 °C and stopped at 180 °C with a ramp rate of 5 °C/min. Figure 3b shows the deposition rates of the Alq3 and TPD molecules as a function of temperature. According to the deposition rates, the molar ratio of Alq3 to TPD in the resultant film was calculated to be 1.6 at the beginning of the deposition process and 1.5 at the end, while the average molar ratio of Alq3 to TPD in the resultant thin films was 1.6.

The as-deposited film was green and transparent, uniformly covering the entire substrate when observed by naked eyes or by using a polarized optical microscope. The resultant codeposited film was 2000 Å. The concentrations of the TPD and Alq3 molecules in the polymer matrix were determined according to their deposition rates. The respective volume percentages of TPD and Alq3 in the resultant film were 12% and 17%. The film color did not change upon annealing at 150 °C for 1.5 h. This annealing process allowed the as-deposited films to transfer, at least partly, from poly(amic acid) to polyimide. The atomic force microscopy results revealed that the surface roughness was 19 nm as deposited and 17 nm after annealing.

**FTIR Results.** Figure 4 shows the FTIR spectra of the green codeposited films before and after curing. The absorption peak at 1650  $\text{cm}^{-1}$  corresponds to the characteristic absorption of the amide carbonyl group of PAA of the as-deposited film.<sup>22</sup> This absorption confirms the formation of the PAA structure, indicating that synthesis of the poly(amic acid) was not disturbed by the codeposition of the TPD and Alq3 molecules. However, since the absorption peaks corresponding to the pure PMDA monomer were also observed at 1780 and 1850  $\text{cm}^{-1}$ ,<sup>23</sup> we could postulate that the as-deposited films may possess some unreacted monomers.

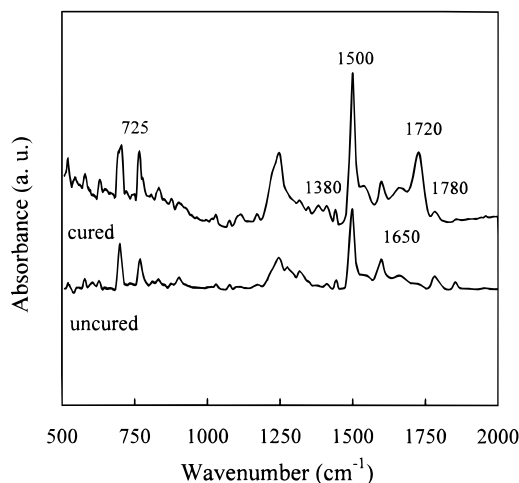


**Figure 4.** FTIR spectrometry results of the resultant thin films before and after curing.

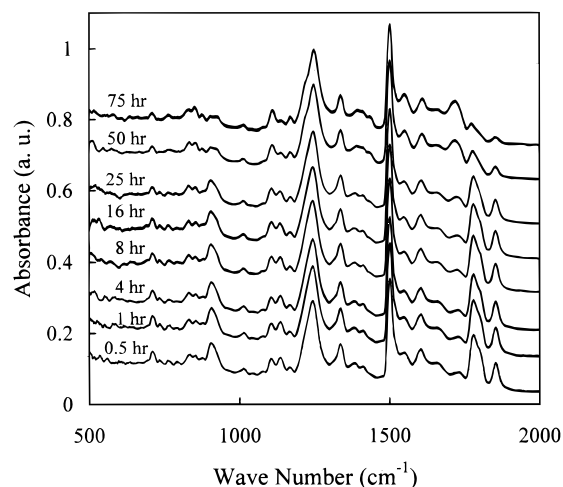


**Figure 5.** FTIR spectra of the as-deposited film after storing in air for various periods of time.

After curing, the imide absorption that had peaked at 725, 1380, 1720, and 1780  $\text{cm}^{-1}$ , respectively, clearly appeared, indicating that the PAA structure had been converted into the PI counterpart.<sup>22</sup> In contrast, the absorption peaks of the unreacted PMDA monomer disappeared altogether. The residual unreacted monomers could have further either reacted or sublimated during the curing process. The peak of the amide at 1650  $\text{cm}^{-1}$ , however, did not diminish completely, suggesting further that some of the PAA chains had not been converted. Higher curing temperatures might have improved the extent of imidization. But, any elevation of the curing temperature should carefully proceed so that the doped molecule does not sublime or degrade thermally.

Degradation of the as-deposited films was observed when they were stored in air. Figure 5 shows the change in FTIR spectra of an as-deposited film with storage time increasing from 0.5 to 75 h. With time on, the characteristic absorption peaks of the dianhydride monomer at 1780 and 1850  $\text{cm}^{-1}$  and that of the amide at 1650  $\text{cm}^{-1}$  decreased, while that of the carboxylic acid at 1725  $\text{cm}^{-1}$  increased. Figure 6 shows with respect to time the variations of the corresponding peak intensities. The decrement of the amide and dianhydride peak intensities indicates a reduction in the unreacted PMDA monomer and previously formed PAA in the films. Both



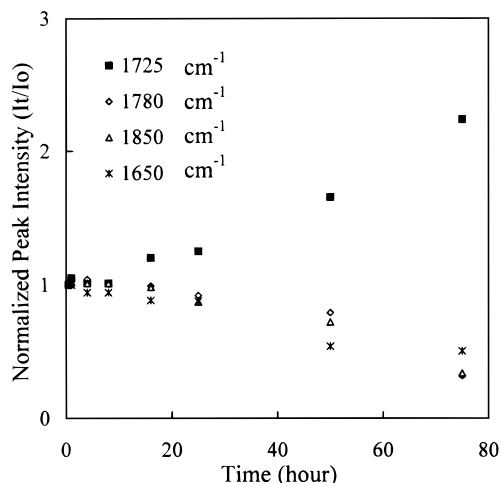


**Figure 6.** Intensity variations of the characteristic FTIR peaks with respect to time of the as-deposited film.

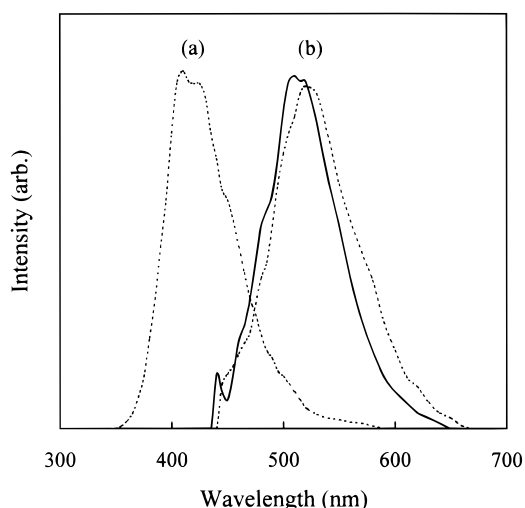


**Figure 7.** Photoluminescence spectra of the (a) TPD- and (b) Alq3-doped polymer thin films (broken lines). Electroluminescence spectra of the TPD- and Alq3-codoped VDP polymer thin film (solid line).

the dianhydride and amide are believed to hydrolyze to their carboxylic acid counterparts, a deduction supported by the increment of the carboxylic acid intensity as seen in the same figure. Hence, hydrolysis can be concluded to be the major cause of the degradation of the as-deposited films stored in air.

**EL Characteristics.** Figure 7 shows the photoluminescence spectra of the TPD-doped and the Alq3-doped polymer thin films. The electroluminescence spectrum for the EL device fabricated is also included in the figure for comparison. The PL spectrum of the TPD-doped thin film exhibited a peak at 410 nm, whereas the Alq3 film exhibited a peak at 520 nm. The EL spectra of the device, however, showed only one peak, at 515 nm, confirming the hole-transporting role of the TPD molecules. The electroluminescence characteristics can therefore be concluded here to be originated from the electronically excited singlet state of Alq3 generated by the recombination of holes and electrons injected.

Figure 8 shows the current–voltage and the electroluminescence (EL) intensity–voltage results of the resultant devices. In the devices, Al was used as a negative electrode (electron-injecting electrode) and ITO

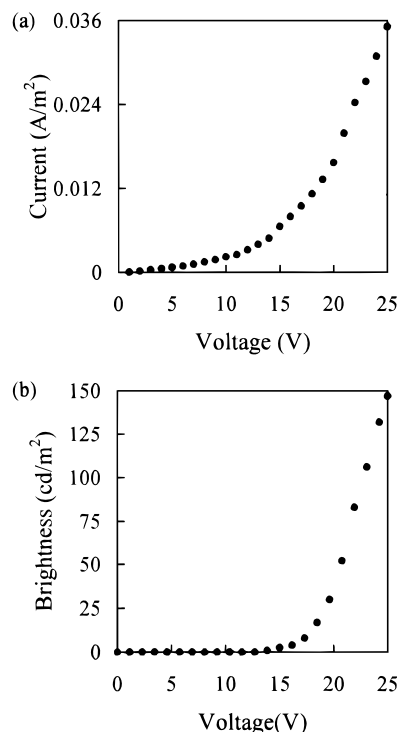


**Figure 8.** (a) Current–voltage characteristics and (b) luminescence intensity–voltage characteristics of the TPD- and Alq3-codoped VDP film.

as a positive electrode (hole-injecting electrode). As shown in Figure 8 the threshold voltage was observed to be 14 V. This corresponded to an electric strength of  $7 \times 10^5$  V cm<sup>-1</sup> for the film. When the applied voltage exceeded the threshold voltage, the EL intensity became proportionally linear to the applied voltage. The EL intensity then was observed to rise from 14 V. This corresponded to a current density of 5 mA/cm<sup>2</sup>. The quantum efficiency of the device was determined to be 0.23% at a driving voltage below 18 V.

**Degradation.** Figure 9a shows luminescence decrement properties resulting from continuous running of the emitting test of the above EL devices, with each data point representing an average of three devices. The test was carried out in air and under a constant current of 21 mA/cm<sup>2</sup>. The initial luminescence was set at 85 cd/m<sup>2</sup> for these testing devices. For the uncured device, the EL intensity rapidly decreased with time and vanished after 52 h, a phenomenon attributed to the moisture-attack-induced degradation of the PAA polymer matrix, as mentioned above. Contrarily, the cured device showed a much better stability: its EL intensity remained at 50% of its original intensity after 112 h. The curing process did improve the films stability, though the film was not fully imidized. In both cases, the luminescence decay rate was directly proportional to the injection current density; the larger the drive current, the greater the rate of decrease in its luminescence. Reduction in the luminescence, in our experiment, was found to be caused also by the formation, growth, and presence of dark nonemissive regions, as reported by Burrows et al. and Fujihira et al.<sup>24,25</sup> The incomplete contact areas (or dark spots) increase in both size and number with the increase of operation time. As a result, the active area of the device decreases and the device internal resistance increases. A higher and higher voltage is hence needed in order to maintain the

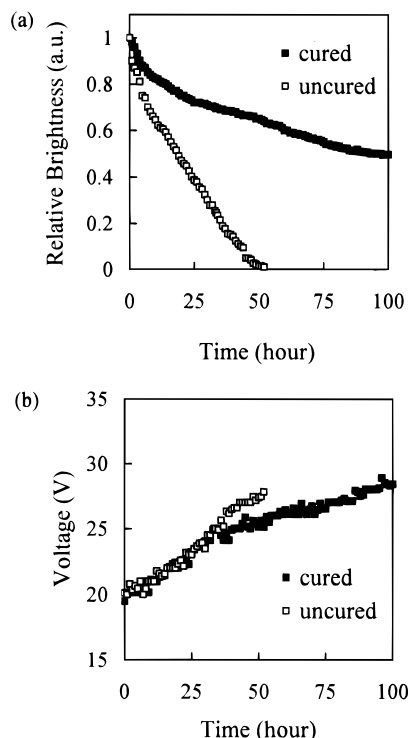


**Figure 9.** EL intensity and applied voltage versus time of an ITO/codeposition film/Al OEL device operated at a constant current of 21 mA/cm<sup>2</sup> under ambient conditions.

constant drive current conditions. The results are shown in Figure 9b.

**Interface Topology Investigation.** Since the delamination process was the most likely cause of the injection barrier in the dark regions observed in the OEL device, the top electrode was subsequently peeled off from the sample to isolate the interface at which the delamination might have occurred.<sup>26</sup> To track the interface topology change during the delamination process, the Al surface on the Al/codeposition film interfacial side was investigated at several stages of life shown in Figure 10. The Al metal in the interfacial side became significantly rough with time. After 75 h of continuous operation, it contained some shaped structures with small spikes and its roughness increased from 17 to 71 nm.

The nonuniform formation of the Al film on the Al/codeposition film interfacial side generated some interfacial gaps and reduced the effective contact area. The interfacial gap reduced the effectiveness of the electric field applied on the device. To keep the same effectiveness, a higher operation voltage was consequently required. The coarse Al metal may have also resulted in the small spikes on the interface, and such spikes caused the device to fail easily upon the application of a small voltage. These results revealed the important effects of the surface topology of the on-top deposited Al metal at the interfacial side on the degradation process of such devices.

## Conclusion

Molecularly doped EL polymer thin films of the single-layer type have been successfully prepared by using vapor deposition polymerization. The EL function was

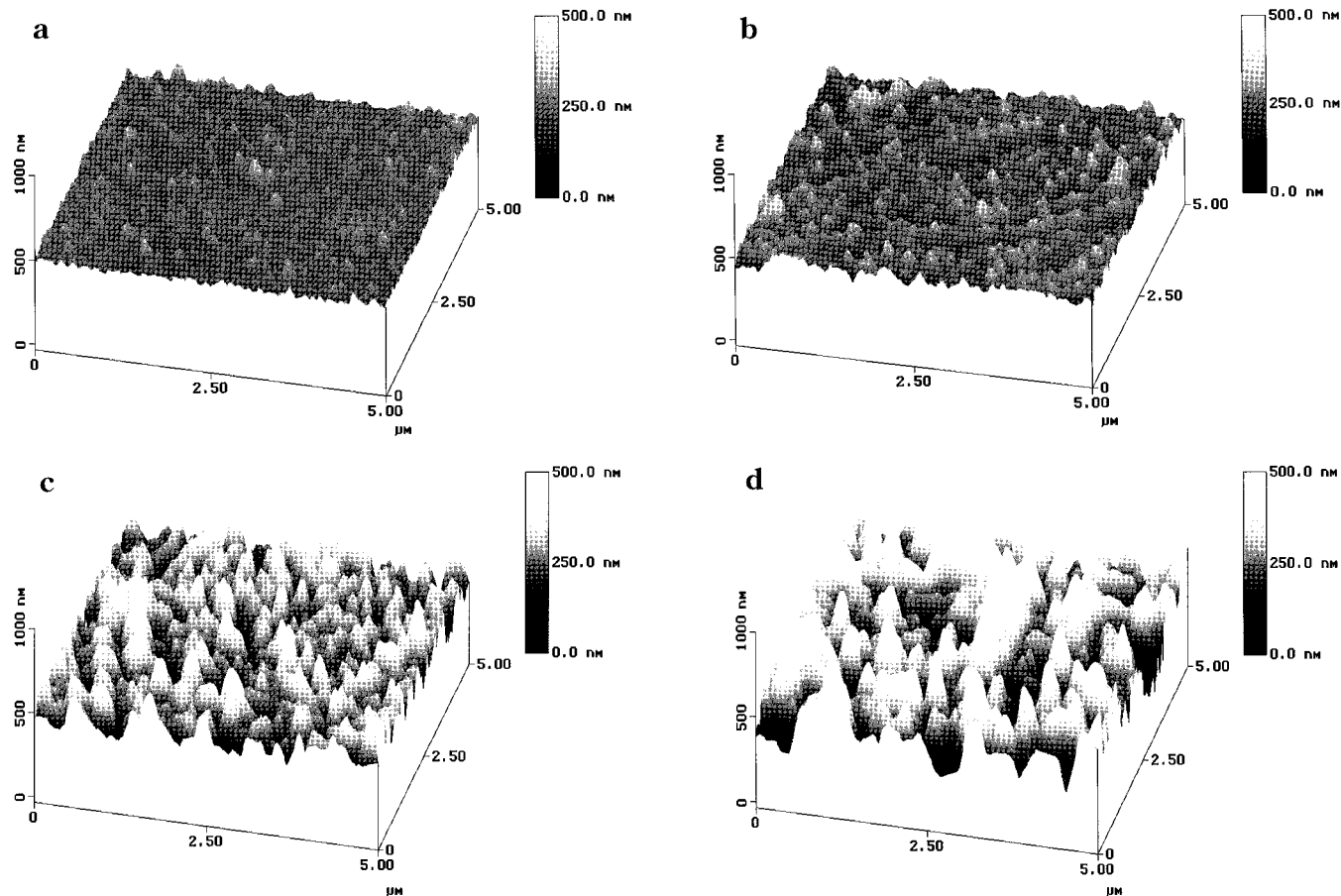


**Figure 10.** AFM images of the Al surface topology on the Al/codeposition film interfacial side for the cured OEL devices after running for (a) 0 h, (b) 25 h, (c) 75 h, and (d) 100 hr.

triggered at a voltage of 14 V. The peak emission wavelength was 515 nm, a green visible light. The uncured poly(amic acid) matrix degraded due to moisture absorption, which in turn resulted in the deterioration of the EL intensity. Curing the specimens at a moderately high temperature had greatly improved the film integrity and likewise the EL characteristics. A higher curing temperature is expected to yield a more thermally stable thin film, providing a more thermally stable OEL-active molecule is available. The novelty of the presented method is in its ease of use. It can be applied to many other fluorescent dye-doped polymer thin film systems, yet without having to go through the hassles of complicated conventional synthesis and fabrication processes.

**Acknowledgment.** We are grateful to the National Science Council, Taiwan, ROC, for the financial support of this work under grants NSC85-2216-E-007-003 and NSC86-2216-E-007-005. We also express our thanks to Mr. J.-H. Lin for his helpful discussion.

## References and Notes

- (1) Tang, C. W.; VanSlyke S. A. *Appl. Phys. Lett.*, **1987**, *51*, 913.
- (2) Adachi, C.; Tokito, S.; Tsutsui, T.; Saito, S. *Jpn. J. Appl. Phys.* **1988**, *27*, L713.
- (3) Kido, J.; Kimura, M.; Nagai, K. *Science* **1995**, *267*, 1332.
- (4) Sheats, J. R.; Antoniadis, H.; Hueschen, M.; Leonard, W.; Miller, J.; Moon, R.; Roitman, D.; Stocking, A. *Science* **1996**, *273*, 884.
- (5) Adachi, C.; Tsutsui, T.; Saito, S. *Appl. Phys. Lett.* **1989**, *55*, 1489.
- (6) Adachi, C.; Nagai, K.; Tamoto, N. *Appl. Phys. Lett.* **1995**, *66*, 2679.
- (7) Matsumura, M.; Akai, T.; Saito, M.; Kimura, T. *J. Appl. Phys.* **1996**, *79*, 264.
- (8) Kido, J.; Kohda M.; Nagai, K. *Appl. Phys. Lett.* **1992**, *61*, 761.
- (9) Kido, J.; Shionoya, H.; Nagai, K. *Appl. Phys. Lett.* **1995**, *67*, 2281.
- (10) Ohmori, Y.; Uchida, M.; Morishima, C.; Fujii, A.; Yoshino, K. *Jpn. J. Appl. Phys.* **1993**, *32*, L1663.
- (11) Wang, G.; Yuan, C.; Wu, H.; Wei, Y. *Jpn. J. Appl. Phys.* **1995**, *34*, L182.
- (12) Wu, C. C.; Sturm, J. C.; Register, R. A.; Tian, J.; Dana, E. P.; Thompson, M. E. *IEEE Trans. Electron Devices* **1997**, *44*, 1269.
- (13) Braun, D.; Heeger, A. J. *Appl. Phys. Lett.* **1991**, *61*, 761.
- (14) Mori, Y. In *Organic Electroluminescent Material and Device*; Miyata, S., Nalwa, H. S., Eds.; Gordon and Breach Publishers: New York, 1997; p 391.
- (15) Tamada, M.; Omichi, H.; Okui, N. *Thin Solid Films* **1995**, *268*, 18.
- (16) Hosokawa, C.; Higashi, H.; Kusumoto, T. U.S. patent No. 5,443,921, 1995.
- (17) Sakakibara, Y.; Iijima, M.; Tsukagoshi, K.; Takahashi, Y. *Jpn. J. Appl. Phys.* **1993**, *32*, L332.
- (18) Takahashi, Y.; Iijima, M.; Oishi, Y.; Kamimoto, M.; Imai, Y. *Macromolecules* **1991**, *24*, 3543.
- (19) Hikita, M.; Yamada, S.; Mizutani, T. *Jpn. J. Appl. Phys.* **1993**, *32*, 2667.
- (20) Salem, J. R.; Sequeda F. O.; Duran J.; Lee, W. Y.; Tang, R. M. *J. Vac. Sci. Technol.* **1986**, *A4*, 369.
- (21) Iijima, M.; Takahashi, Y.; Inagawa, K.; Itoh, A. *J. Vac. Sci. Jpn.* **1985**, *28*, 437.
- (22) Iijima, M.; Takahashi, Y. *Macromolecules* **1989**, *22*, 2944.
- (23) Iijima, M.; Takahashi, Y.; Oishi, Y.; Kakimoto, M.; Imai, Y. *J. Polym. Sci.* **1991**, *A29*, 1717.
- (24) Burrows, P. E.; Bulovic, V.; Forrest, S. R.; Sapochak, S.; Mccarty, D. M.; Thompson, M. E. *Appl. Phys. Lett.* **1994**, *65*, 2922.
- (25) Fujihira, M.; Do, L. M.; Koike, A.; Han, E. M. *Appl. Phys. Lett.* **1996**, *68*, 1787.
- (26) Sato, Y.; Kanai, H. *Mol. Cryst. Liq. Cryst.* **1994**, *253*, 143.

MA9807771